Bioorg. Med. Chem. 38 (2021) 116139

Contents lists available at ScienceDirect

Bioorganic & Medicinal Chemistry

journal homepage: www.elsevier.com/locate/bmc

Ximaoglaucumins A – F, new cembranoids with anti-inflammatory activities from the South China Sea soft coral *Sarcophyton glaucum*

Shou-Mao Shen [a,b,1], Wang-Sheng Li [b,c,1], Xun Ding [d,e], Hui Luo [c,*], Hai-Yan Zhang [d,e,*], Yue-Wei Guo [a,b,*]

[a] School of Chinese Materia Medica, Nanjing University of Chinese Medicine, Nanjing 210023, China
[b] State Key Laboratory of Drug Research, Shanghai Institute of Materia Medica, Chinese Academy of Sciences, 555, Zu Chong Zhi Road, Zhangjiang Hi-Tech Park, Shanghai 201203, China
[c] Marine Biomedical Research Institute, Guangdong Key Laboratory for Research and Development of Natural Drugs, Guangdong Medical University, Zhanjiang 524023, China
[d] University of Chinese Academy of Sciences, No. 19A Yuquan Road, Beijing 100049, China
[e] CAS Key Laboratory of Receptor Research, Shanghai Institute of Materia Medica, Chinese Academy of Sciences, Shanghai 201203, China

ARTICLE INFO

Keywords:
Soft coral
Sarcophyton glaucum
Cembranoids
Anti-inflammation

ABSTRACT

Six new cembrane-type diterpenoids, namely ximaoglaucumins A–F (**1**–**6**), along with fifteen known related ones (**7**–**10** and **14**–**24**), have been isolated from the soft coral *Sarcophyton glaucum* collected off the Ximao Island in the South China Sea. Their structures, including absolute stereochemistry, were elucidated by extensive spectroscopic analysis, quantum mechanical nuclear magnetic resonance (QM-NMR) methods, X-ray diffraction analysis, chemical methods, as well as comparison with the reported data in the literature. Further, detailed analysis of spectroscopic data of **7** not only clarified the confusions regarding **7**, **11** (sarcophytolol) and **12**/**13** (sarcotrocheliol) in the literature, but also led to revise the structure of **11**, which was mis-assigned due to careless/erroneous interpretation of the 2D NMR spectra, and to correct the structures of **12**/**13**, which were both wrongly depicted. In *in vitro* bioassay, compounds **8** and **20** exhibited potent inhibitory effects on lipopolysaccharide (LPS)-induced inflammatory responses in BV-2 microglial cells.

1. Introduction

Soft corals (phylum Cnidaria) are an important group of marine invertebrates widely distributed in the coral reefs of the world oceans. Of them, the animals belonging to the genus *Sarcophyton* (class Anthozoa, subclass Octocorallia, order Alcyonaceae, family *Alcyoniidae*) are very prolific, in particular, widely inhabited in South China Sea. Literature survey revealed that over 40 species of the *Sarcophyton* soft corals have been chemically investigated, and numerous structurally diverse and biologically active secondary metabolites, of which dominately cembrane-type diterpenoids, were isolated and characterized.[1–3] Moreover, some metabolites isolated from animals of the title genus exhibited a wide spectrum of biological activities including neuroprotective, ichthyotoxic, cytotoxic, antiviral, antifouling, and anti-inflammatory properties.[3]

Our group has long been engaged in the searching for novel bioactive secondary metabolites from Chinese marine organisms,[2–5] especially Cnidarian animals.[6–8] In the last decade, in the course of our continuous efforts towards searching for bioactive metabolites from Hainan soft corals, nine *Sarcophyton* species have been chemically investigated, and a lot of novel terpenoids with intriguing structures and some of them with unprecedented structural frameworks were discovered.[9–12] *S. glaucum*, collected off the coast of Lingshui Bay, Hainan Province, China, had been investigated in 2009 by our group and a series of novel cembranolides bearing uncommon five-membered lactone rings were isolated and characterized.[13] Recently, the same animal was encountered off the Ximao Island, Hainan Province, China. The chemical investigation on the crude Et_2O extract of this collection has now resulted in the isolation of six new cembranoids, named ximaoglaucumins A–F (**1**–**6**), and fifteen known related ones (**7**–**10** and **14**–**24**)

* Corresponding author at: School of Chinese Materia Medica, Nanjing University of Chinese Medicine, Nanjing 210023, China and State Key Laboratory of Drug Research, Shanghai Institute of Materia Medica, Chinese Academy of Sciences, Shanghai 201203, China (Y.-W. Guo).
E-mail addresses: luohui@gdmu.edu.cn (H. Luo), hzhang@simm.ac.cn (H.-Y. Zhang), ywguo@simm.ac.cn (Y.-W. Guo).
[1] These authors contributed equally to this work.

https://doi.org/10.1016/j.bmc.2021.116139
Received 9 December 2020; Received in revised form 5 March 2021; Accepted 23 March 2021
Available online 2 April 2021

(Fig. 1). Herein, we report the isolation, structural elucidation, and biological evaluation of these isolates.

2. Results and discussion

2.1. Structural elucidation of isolates

The frozen bodies of *S. glaucum* were cut into pieces and extracted exhaustively with acetone. The acetone extract was devided into Et_2O-soluble and BuOH-soluble portions. The Et_2O-soluble portion was repeatedly chromatographed over silica gel, Sephadex LH-20 and reversed-phase (RP)-HPLC to afford twenty-one pure compounds (**1**–**10** and **14**–**24**).

Compounds **8**–**10** and **14**–**24** were readily identified as (+)-sarcophytol A (**8**),[14] sarcophytol H (**9**),[15,16] (–)-marasol (**10**),[16,17] cembrene C (**14**),[17] alcyonol-B (**15**),[18] (+)-sarcophytol A acetate (**16**),[17] 14-*O*-acetylsarcophytol B (**17**),[19] sarcophytol N (**18**),[15] (+)-11,12-epoxysarcophytol A (**19**),[20] sarcophytol B (**20**),[15] sarcophytol I (**21**),[15] sarcophytol G (**22**),[15] 4-epiisocembrol (**23**)[21] and (–)-(*R*)-nephthenol (**24**),[22] respectively, by comparison of their NMR data (Table S1, Supporting Information) and optical rotation values with those reported in the literature. In addtion, the full structure of compound **8** (Fig. 2), which was previously isolated from the same species collected off the Ishigaki Island, Okinawa,[14] was unambiguously confirmed by X-ray diffraction analysis using Cu Kα radiation (λ = 1.54178 Å) [Flack parameter: 0.05 (12)], since it was crystallized from petroleum ether (PE)/CH_2Cl_2/MeOH (2:1:1) at room temperature (RT) in present study.

Among the six new cembranoids, compounds **1**–**5** showed the NMR data characteristic for the conjugated diene moiety bearing an isopropyl group at C-1 and a methyl group at C-4 of cembranoid framework, like those of co-occurring **8** and **9**, while the NMR spectra of **6** was quite different from those of **1**–**5** displaying the presence of ether ring in its molecule. The structural elucidation of these metabolites is described as follows.

Compound **1** was obtained as an optically active colorless oil. Its molecular formula was deduced to be $C_{22}H_{34}O_3$ on the basis of the HRESIMS pseudo-molecular ion peak at *m/z* 369.2409 ($[M + Na]^+$, calcd 369.2400). The IR absorption bands at 3440 and 1738 cm^{-1}

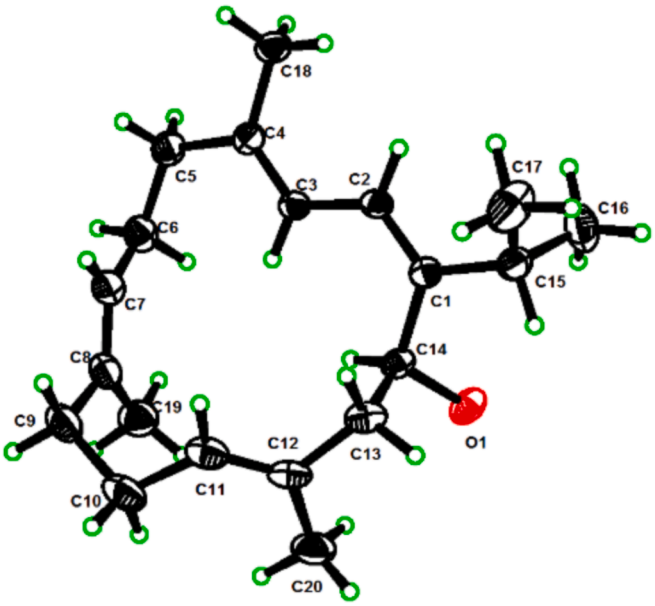

Fig. 2. ORTEP drawing of (+)-sarcophytol A (**8**).

implied the presence of hydroxyl and ester carbonyl groups. Careful comparison of the NMR data of **1** (Tables 1 and 2) and **8**[14] revealed that the main differences between them happened at C-20 and its neighboring carbons (*e.g.*, C-11, C-12, C-13), indicating the acetoxylation occurring at the C-20 of **1**. In fact, due to the acetoxylation, the ^1H NMR signal of the C-20 methyl in **8** was disappeared, and the ^{13}C NMR chemical shifts of C-20 and C-11 were apparently downfield shifted from δ_C 18.4 and 125.5 in **8** to δ_C 63.4 and 131.9 in **1**, respectively, according to the 58 mass units difference between the molecular weights of **1** and **8**. Compound **1** contains only one chiral center at C-14, of which, the absolute stereochemistry was deduced to be *S*, the same as that of **8**, based on the biogenetic consideration. However, in order to secure the absolute configuration of C-14, the modified Mosher's method was

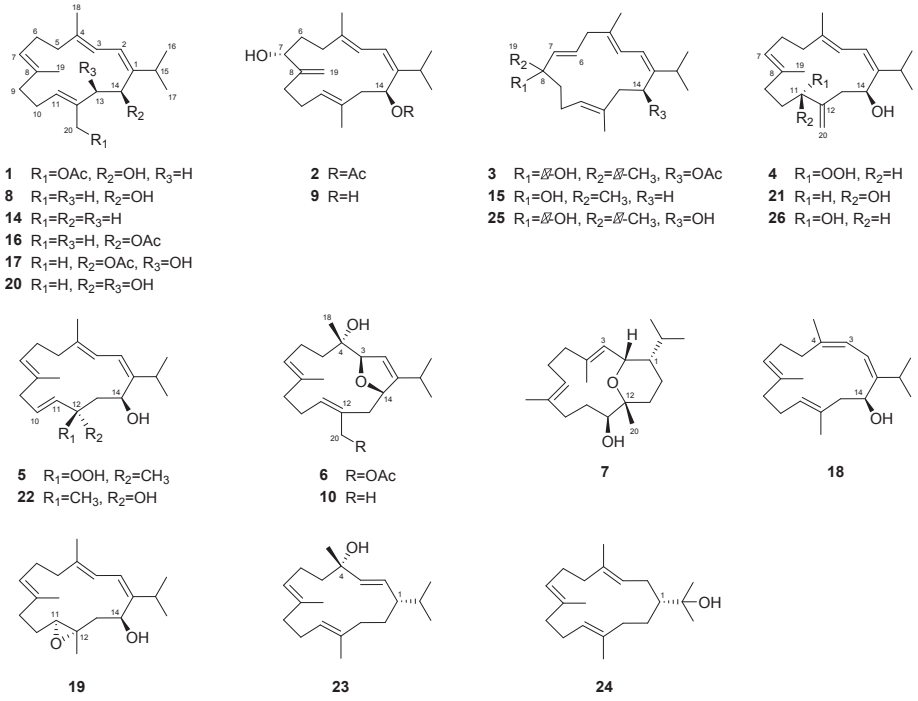

Fig. 1. Chemical structures of compounds **1**–**10** and **14**–**26**.

Table 1
^{1}H NMR (δ_H, mult., J in Hz) data of compounds **1**–**6** in $CDCl_3$.

No.	1[a]	2[b]	3[b]	4[b]	5[b]	6[b]
1	–	–	–	–	–	–
2	6.15, d (11.5)	6.22, d (11.4)	6.11, d (11.4)	6.01, d (10.8)	6.05, d (10.8)	5.42,br s
3	5.97, d (11.5)	5.98, d (11.4)	5.99, dd (11.4, 1.2)	5.90, d (10.8)	5.90, d (10.8)	4.61, d (5.4)
5a	2.18[c], overlap	2.29[d], overlap	2.80, dd (16.8, 6.6)	2.22[f], overlap	2.19 [h], overlap	1.88, m
5b	2.08, m	2.25[d], overlap	2.69, dd (16.8, 6.6)	2.08 [g], overlap	2.09, m	1.56, m
6a	2.20[c], overlap	2.06, m	5.71, dt (15.6, 6.6)	2.18[f], overlap	2.16 [h], overlap	2.37[i], overlap
6b	2.13[c], overlap	1.77, m		2.18[f], overlap	2.16 [h], overlap	2.14[j], overlap
7	4.97, t (6.0)	3.86, t (6.0)	5.59, d (15.6)	5.14, t (7.2)	5.13, t (6.6)	5.29, dd (10.8, 3.0)
9a	2.18[c], overlap	2.48[e], overlap	1.91, m	2.22[f], overlap	2.74, dd (13.8, 7.2)	2.15[j], overlap
9b	2.03, m	2.20[d], overlap	1.72, m	2.01, m	2.69, dd (13.8, 7.2)	2.15[j], overlap
10a	2.29, m	2.25[d], overlap	2.17, m	1.77, m	5.83, dt (15.6, 7.2)	2.41, m
10b	2.17[c], overlap	2.13, m	2.17, m	1.62, m		1.93, m
11	5.30, dd (7.5, 5.5)	5.25, t (6.0)	5.31, t (6.0)	4.42, dd (7.8, 4.8)	5.47, d (15.6)	5.47, dd (10.2, 3.0)
12	–	–	–	–	–	–
13a	2.44, m	2.47[e], overlap	2.50, dd (13.8, 6.0)	2.45, dd (13.8, 9.6)	1.99, dd (13.8, 8.4)	2.45, m
13b	2.44, m	2.24[d], overlap	2.26, dd (13.8, 6.0)	2.08 [g], overlap	1.80, dd (13.8, 1.2)	2.34[i], overlap
14	5.01, dd (8.5, 5.0)	5.86, dd (10.8, 3.6)	5.63, dd (6.0, 6.0)	4.96, dd (9.6, 3.6)	4.78, dd (8.4, 1.2)	4.86, dd (5.4, 5.4)
15	2.59, m	2.52, m	2.38, m	2.68, m	2.56, m	2.30, m
16	1.11, d (7.0)	1.04, d (6.6)	1.06, d (7.2)	1.11, d (7.2)	1.11, d (7.2)	1.03, d (6.6)
17	1.03, d (7.0)	1.14, d (6.6)	1.10, d (7.2)	1.09, d (7.2)	1.10, d (7.2)	1.16, d (6.6)
18	1.74, s	1.76, s	1.77, s	1.74, s	1.74, s	1.01, s
19a	1.46, s	5.08, d (1.2)	1.33, s	1.55, s	1.60, s	1.57, s
19b		5.02, br s				
20a	4.66, d (12.0)	1.53, s	1.52, s	5.24, brs	1.53, s	4.63, d (12.0)
20b	4.43, d (12.0)			5.10, brs		4.32, d (12.0)
OAc	2.05, s	2.02, s	2.07, s			2.04, s
OOH				8.14, brs	7.23, brs	

[a] Spectra were recorded at 500 MHz for ^{1}H NMR; [b] Spectra were recorded at 600 MHz for ^{1}H NMR; [c-j] These assignments may be interchanged.

Table 2
^{13}C NMR data (δ in ppm) of compounds **1**–**6** in $CDCl_3$.[a.]

No.	1	2	3	4	5	6
1	146.7, qC	143.0, qC	145.0, qC	148.0, qC	148.4, qC	150.7, qC
2	120.9, CH	121.7, CH	112.0, CH	118.7, CH	119.5, CH	119.7, CH
3	121.1, CH	120.4, CH	121.2, CH	121.5, CH	120.6, CH	87.3, CH
4	136.7, qC	136.6, qC	137.2, qC	136.4, qC	137.0, qC	74.8, qC
5	39.7, CH_2	35.1, CH_2	41.4, CH_2	40.1, CH_2	38.9, CH_2	38.6, CH_2
6	25.7, CH_2	31.3, CH_2	125.6, CH	25.7, CH_2	25.0, CH_2	25.5, CH_2
7	125.4, CH	69.1, CH	139.4, CH	125.8, CH	125.7, CH	129.0, CH
8	134.3, qC	149.6, qC	73.2, qC	133.9, qC	134.5, qC	132.1, qC
9	38.7, CH_2	34.0, CH_2	41.6, CH_2	34.7, CH_2	42.9, CH_2	39.7, CH_2
10	24.4, CH_2	25.0, CH_2	23.3, CH_2	29.9, CH_2	132.8, CH	22.2, CH_2
11	131.9, CH	127.7, CH	128.8, CH	83.0, CH	132.5, CH	138.4, CH
12	130.6, qC	131.2, qC	132.4, qC	146.9, qC	85.4, qC	129.0, qC
13	40.3, CH_2	42.6, CH_2	45.2, CH_2	43.8, CH_2	43.2, CH_2	38.7, CH_2
14	69.9, CH	74.0, CH	75.4, CH	68.3, CH	67.5, CH	84.4, CH
15	27.2, CH	28.1, CH	30.3, CH	28.3, CH	27.8, CH	26.5, CH
16	25.5, CH_3	25.3, CH_3	23.6, CH_3	24.4, CH_3	26.1, CH_3	22.2, CH_3
17	24.4, CH_3	23.9, CH_3	23.1, CH_3	23.7, CH_3	24.4, CH_3	21.0, CH_3
18	16.5, CH_3	16.8, CH_3	18.0, CH_3	16.4, CH_3	17.2, CH_3	23.9, CH_3
19	15.6, CH_3	111.1, CH_2	28.9, CH_3	16.1, CH_3	16.7, CH_3	15.7, CH_3
20	63.4, CH_2	18.7, CH_3	17.4, CH_3	113.3, CH_2	21.8, CH_3	63.3, CH_2
OAc	171.2, qC	170.2, qC	170.4, qC			171.2, qC
	21.1, CH_3	21.5, CH_3	21.4, CH_3			21.2, CH_3

[a] Spectra were recorded at 125 MHz for ^{13}C NMR.

applied. Thus, two aliquots of compound **1** were treated with (*R*)-(–) and (*S*)-(+)-α-methoxy-α-(triflurometh yl) phenylacetyl choloride (MTPA-Cl) in dry pyridine at RT, yielding the corresponding (*S*)- (**1a**) and (*R*)- (**1b**) MTPA esters, respectively. Assignment of the ^{1}H NMR signals of the MTPA esters was achieved by careful analyzing their ^{1}H NMR spectra. The ^{1}H NMR chemical shift differences [$\Delta\delta_H = \delta_{(S)\text{-ester}} - \delta_{(R)\text{-ester}}$] of the protons surrounding the C-14 are shown in Fig. 3. The negative $\Delta\delta_H$ values were recorded for the selected protons H_2-13, H_2-20, H-11 and OAc, whereas positive $\Delta\delta_H$ values were observed for the selected protons H-2, H-15, H_3-16, H_3-17 and H_3-18. According to the Mosher's rule,[23] the absolute configuration at C-14 in **1** was determined as expected *S*. In light of these evidences, the structure of **1** was unambiguously elucidated as depicted in Fig. 1, and named ximaoglaucumin A.

Compound **2** was also obtained as a colorless oil. Its molecular formula, $C_{22}H_{34}O_3$, consistent with six degrees of unsaturation, was determined by the HREIMS molecular ion peak at *m/z* 346.2497 (M^+, calcd 346.2502). The IR spectrum of **2**, like that of **1**, also displayed typical absorption bands indicative of hydroxyl (3444 cm^{-1}) and ester carbonyl (1739 cm^{-1}) groups. Overall comparison of the ^{1}H and ^{13}C NMR data of **2** (Tables 1 and 2) with those of co-occurring sarcophytol H (**9**), previously reported from the same species of Okinawa origin,[15,16] revealed that the differences between them mainly happened at C-14. In

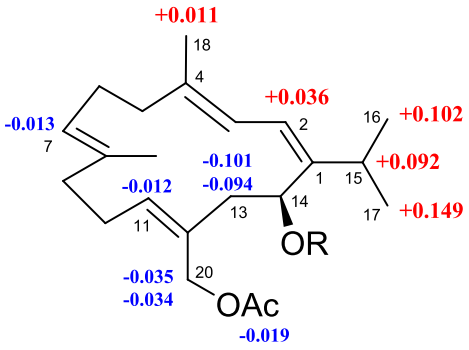

1 R=H; **1a** R=*S*-MTPA; **1b** R=*R*-MTPA

Fig. 3. $\triangle\delta_H$ values (δ_S-δ_R) (ppm) for the protons near C-14 of (*S*)- and (*R*)-MTPA esters of **1**.

fact, due to the acetylation of the hydroxyl group at C-14, the ^{13}C NMR chemical shift of C-14 was obviously downfield shifted (δ_C 71.9 in **9** and 74.0 in **2**), whereas the chemical shifts of C-13 and C-1 of **2** were reasonably upfield shifted from δ_C 45.7 and 147.5 in **9** to δ_C 42.6 and 143.0 in **2**, respectively, according to the 42 mass units difference between the molecular weights of **2** and **9**. There are two chiral centers at C-7 and C-14 in **2**. The absolute configuration of C-7 should be the same as that of **9** due to their highly similar NMR chemical shifts surrounding C-7, whereas the absolute configuration of C-14 was tentatively assigned as *S*, the same as that of **9**, based on the biogenetic consideration. Compound **2** is a C-14 acetyl derivative of **9**, named ximaoglaucumin B.

Compound **3** has the same molecular formula ($C_{22}H_{34}O_3$) as that of **2**, implying **3** is isomeric with **2**. IR spectrum of **3**, like **2**, also showed the diagnostic absorption bands of hydroxyl and ester carbonyl groups. Detailed analysis of the ^{1}H and ^{13}C NMR spectra of **3** (Tables 1 and 2) and comparing with those of **2** revealed that the main differences between them happened at C-6 to C-9 and C-8 to C-19 segments. The appearance of an oxygenated quaternary carbon signal at δ_C 73.2 and a methyl signal at δ_C 28.9, accompanying with the disappearance of the typical ^{13}C NMR signals for the exocyclic olefin at $\Delta^{8,19}$ in **2** clearly indicated the hydroxylation occurred at C-8. Further, the characteristic NMR signals of a *trans*-disubstituted double bond [δ_H 5.71 (1H, dt, J = 15.6, 6.6 Hz, H-6), 5.59 (1H, d, J = 15.6 Hz, H-7)] in **3**, combined with the clear proton sequence of H_2-5 (δ_H 2.80, 2.69)/H-6 (δ_H 5.71)/H-7 (δ_H 5.59) displayed in the ^{1}H-^{1}H COSY spectrum, suggested the location of the double bond at $\Delta^{6,7}$ in **3**. The HMBC cross peaks (Fig. 4) observed from H-6/H-10 (δ_H 2.16) to C-8 (δ_C 73.2), and from H_3-19 (δ_H 1.33) to C-7 (δ_C 139.4)/C-8 confirmed the presence of the partial structure from C-6 to C-8 in **3**.

There are two stereogenic centers (C-8 and C-14) in the structure of **3**. The absolute configuration at C-14 was immediately assigned as *S*, the same as that of **2**, through direct comparison of their NMR data and biogenetic consideration. The determination of the C-8 configuration was somewhat difficult. Moreover, the two chiral centers C-14 and C-8 were somewhat remote, preventing the establishment of their relative configuration by NOE correlations, as shown in a computer-generated 3D drawing (Fig. 5). However, a literature survey revealed that **3** is formally an acetyl derivative of sarcophytol R (**25**), a known cembranoid previously isolated from the title animal collected from Ishigaki Island, Okinawa.[24] In order to establish the structural relationship of **3** and model compound **25**, compound **3** was treated with KOH in CH_3OH for 3 h at RT (Scheme 1), and the expected deacetyl product was obtained and its identity with **25** was confirmed by showing the same physical and chemical data as those of sarcophytol R.[24] In light of these observations, the full structure of compound **3** was unambiguously established as depited in Fig. 1.

Compound **4**, an optically active colorless oil, displayed a molecular formula of $C_{20}H_{32}O_3$ as established by the HRESIMS ion peak at *m/z* 343.2245 ([M + Na]$^+$, calcd 343.2244), indicating five degrees of unsaturation. The ^{1}H and ^{13}C NMR data of **4** (Tables 1 and 2) were very similar to those of co-isolated sarcophytol I (**21**), previously isolated from the title animal of Okinawa origin,[15] except for the signals assigned to C-11 and its neighboring carbons (*e.g.*, C-10 and C-12), where the hydroxyl group in **21** was replaced by a hydroperoxy group in **4**, In fact, due to the hydroperoxy group at C-11, the δ_C value of C-11 (δ_C 83.0) was apparently downfield shifted ($\Delta\delta$ = +11.9 ppm), whereas δ_C values of C-10 (δ_C 29.9) and C-12 (δ_C 146.9) were reasonably upfield shifted ($\Delta\delta$ = –3.2 and –3.3 ppm, respectively) compared to those of **21**, according to 16 mass units difference between their molecular weights. The obvious HMBC correlations (Fig. 4) from H-13 (δ_H 2.45)/H-9 (δ_H 2.01) to C-11, and from H-11 (δ_H 4.42)/H-13 to C-20 (δ_C, 113.3) further secured the connection of the hydroperoxy group to C-11.

Further literature survey revealed that **4** was actually a peroxidation derivative of sarcophytol E (**26**).[15,25] Since the absolute configuration of **26** was established previously by chemical conversion,[15,25] a chemical reaction aiming to elucidate the absolute stereochemistry of **4** was performed. Thus, **4** was treated with triphenylphosphine in CH_2Cl_2 for 1 h at RT (Scheme 2) yielding the expected 11-peroxyhydroxyl reduction product **26**. Therefore, the full structure of **4** was unambiguously established as depicted in Fig. 1, named ximaoglaucumin D.

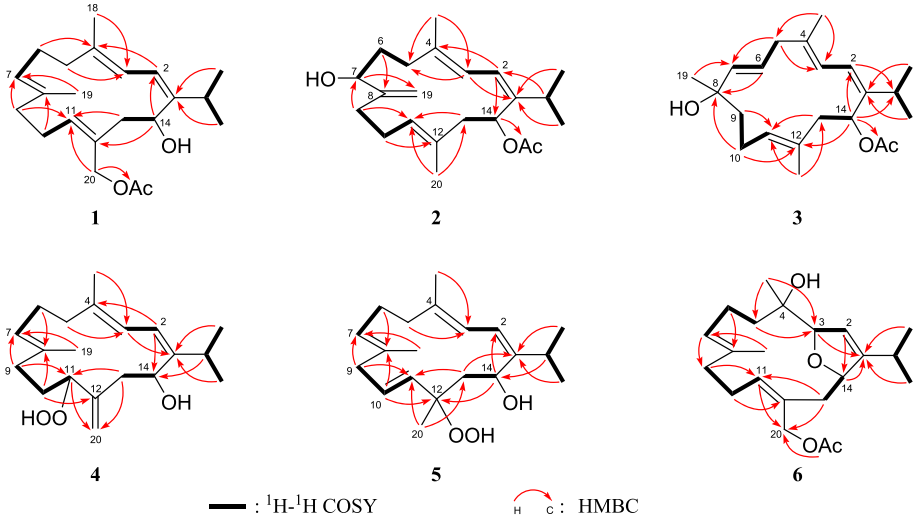

Fig. 4. ^{1}H-^{1}H COSY and key HMBC correlations of compounds **1**–**6**.

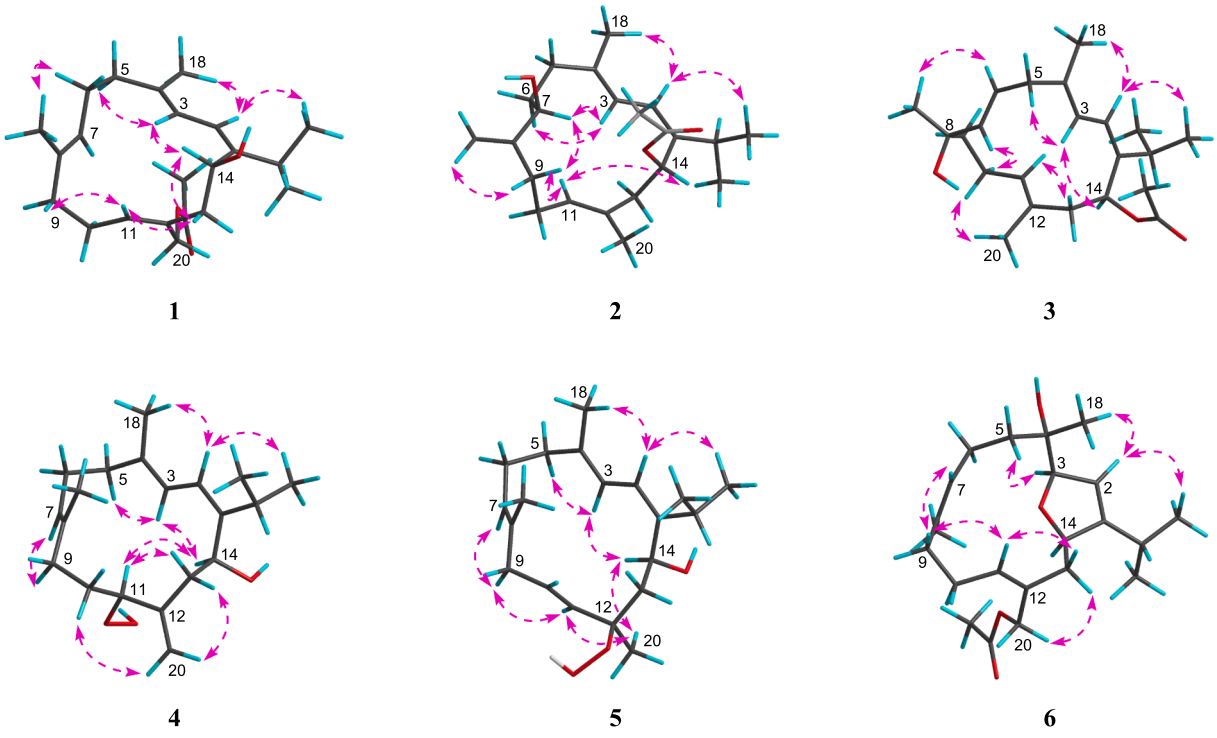

Fig. 5. NOESY correlations of compounds **1**–**6**.

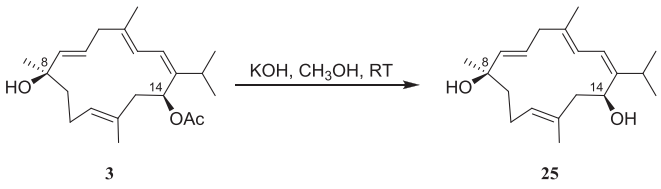

Scheme 1. Chemical conversion of ximaoglaucumin C (**3**) to sarcophytol R (**25**).

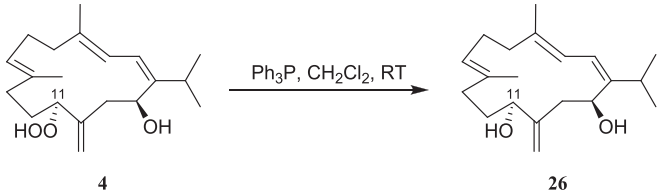

Scheme 2. Chemical conversion of ximaoglaucumin D (**4**) to sarcophytol E (**26**).

Ximaoglaucumin E (**5**) was obtained as a colorless oil. Its molecular formula was established as $C_{20}H_{32}O_3$ on the basis of the HRESIMS pseudo-molecular ion peak at *m/z* 343.2252 ([M + Na]$^+$, calcd 343.2244). The overall NMR data of **5** (Tables 1 and 2) were strongly reminiscent of those of co-occurring sarcophytol G (**22**), previously isolated from the title animal of Okinawa origin,[15] with the main differences at C-12 and its adjacent atoms. The δ_C value of C-12 was visibly downfield shifted from 74.2 in **22** to 85.4 in **5**, whereas the δ_C values of C-11, C-13 and C-20 were all reasonably upfield shifted from 137.5, 46.3 and 30.8 in **22** to 132.5, 43.2 and 21.8 in **5**, respectively, indicating that the hydroxyl group at C-12 in **22** should be replaced by a hydroperoxy group in **5**, according to 16 mass units difference between their molecular weights. The observed HMBC correlations (Fig. 4) from H-10 (δ_H 5.83)/H-14 (δ_H 4.78) to C-12 (δ_C 85.4), and from H_3-20 (δ_H 1.53) to C-11 (δ_C 132.5)/C-13 (δ_C 43.2) further confirmed the planar structure of **5**.

Now, the remaining task is to determine the absolute stereochemistry of **5**. By analog to **4**, we tried to apply the triphenylphosphine method, but unfortunately, the reaction of **5** with triphenylphosphine did not occur, preventing us from assigning rigorously the stereochemistry at the chiral centers C-12 and C-14. To determine the relative configuration of C-12 and C-14, the newly emerged quantum mechanical-nuclear magnetic resonance (QM-NMR) methods were carried out, since the QM-NMR approaches have been widely used to address complex stereo chemical problems of nature products by comparing experimental and computed values.[26] First, conformational searches on the possible candidate stereoisomers (**5a**: 12*R**,14*S** and **5b**: 12*S**,14*S**) were performed. Afterward, geometrical optimizations at the DFT level for conformers above 1% Boltzmann population were undertaken using the B3LYP functional with the 6-31G* basis set, followed by NMR calculations at the PCM/mPW1PW91/6-31+G** level, as recommended for DP4 +.[27] NMR shielding constants (σ) were calculated using the GIAO approach. Finally, shielding constants were averaged over the Boltzmann distribution obtained for each isomer and correlated with the experimental data.[26,28] As a result, the calculation revealed that the experimentally observed NMR data for compound **5** gave better match of 100% with the 12*R**,14*S** isomer (see the Supporting Information for details). Moreover, the absolute configuration of C-14 in **5** was suggested to be *S*, the same as co-occurring **1**–**4** and **8**, by comparing their almost identical positive Cotton effects at 245 nm in ECD spectra. As a consequence, the absolute configuration of **5** was tentatively deduced as 12*R*,14*S*.

Ximaoglaucumin F (**6**) was also isolated as an optically active colorless oil, $[\alpha]^{20}_D$ –121.4 (*c* 0.14, MeOH). Its molecular formula was determined as $C_{22}H_{34}O_4$ by HREIMS molecular ion peak at *m/z* 362.2456 (M$^+$, calcd 362.2452), indicating six degrees of unsaturation. The IR spectrum showed the presence of a hydroxyl group (3452 cm^{-1}) and ester carbonyl (1737 cm^{-1}) group. A careful analysis of its NMR spectra revealed that the NMR spectroscopic features of **6** (Tables 1 and 2) extremely resembled those of co-occurring model compound (–)-marasol (**10**).[16,17] In fact, the only difference between compounds **6** and **10** happened at the C-20 position, where the CH_3-20 in **10** was acetoxylated. The presence of an acetoxyl group at C-20 was confirmed

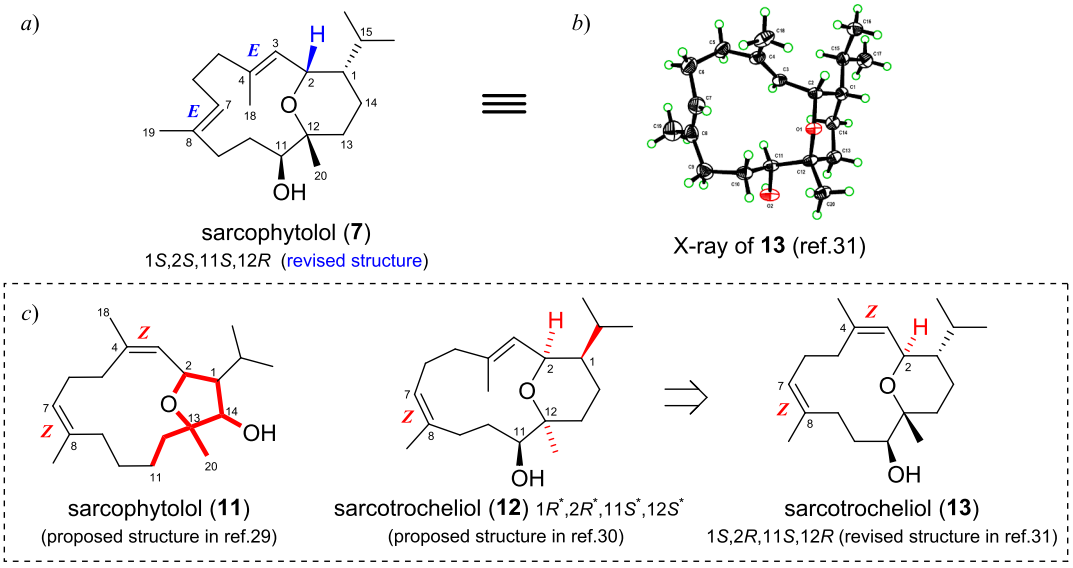

Fig. 6. *a*) Revised structure of sarcophytolol (**7**). *b*) ORTEP drawing of sarcotrocheliol (**13**). *c*) Chemical structures of **11**–**13** in refs. 29–31.

by direct comparison of the NMR data of **6** (Table 2) with those of above elaborated compound **1**. Finally, extensive interpretation of 2D NMR spectra (^{1}H-^{1}H COSY, HSQC, HMBC and NOESY) (Figs. 4 and 5) allowed to complete the full structure of **6** as depicted in Fig. 1. Analogous with the pair compounds of **1** and **8**, compound **6** is a 20-acetoxylation derivative of **10**.

The structural elucidation of compound **7** is somewhat complicated worthing to discuss. **7** was initially identified as sarcophytolol (**11**) (Fig. 6),[29] a cembranoid previously isolated from the same species but collected off the coast of Jeddah, Saudi Arabia in the Red Sea in 2014 by A. Abdel-Lateff *et al*, since both compounds shared almost identical physical and chemical data (Table 3) with only differences on the assignments for C-9–C14, C-18 and C-20. Surprisingly, further literature survey disclosed another related compound **12**, namely sarcotrocheliol (Fig. 6),[30] previously isolated from *S. trocheliophorum* of Jeddah origin by W. M. Alarif *et al*. Interestingly, the proposed structure of **12** was successively revised as **13** (Fig. 6),[31] which was also isolated from *S. trocheliophorum* but collected off the coast of Hurghada, Egypt, and whose structure was secured by X-ray diffraction analysis (Fig. 6) by M. Shaaban *et al* in 2019. So, it is quite sure that all of these four structures (**7** and **11**–**13**) should be the same compound! Overall comparison of ^{1}H and ^{13}C NMR data of **7** with those of **13** (Table 3) confirmed their identity. However, it needs to point out that both the structures of **12**/**13** were erroneously depicted in the refs. 30 and 31. Even worse case was the structural elucidation of **11**. Since its structure was published on an esteemed international journal, a very careful and rigorous comparison of the ^{1}H and ^{13}C NMR data including 2D NMR spectra of **7** (Figures S53–56, Supporting Information) with those of **11** (provided in supplementary data related to ref. 29) was carried out. Surprisingly, we did observe a series of apparent differences between them. Firstly, the ^{1}H and ^{13}C NMR assignments for the methyls at C-18 and C-20 of **11** were obvious mistakes due to their careless analysis of HSQC spectrum (the former: C-18 corresponding to the δ_C 15.2, δ_H 1.64, and C-20 corresponding to the δ_C 24.4, δ_H 1.02; the latter: C-18 corresponding to δ_C 24.2, δ_H 1.65, and C-20 corresponding to the δ_C 15.1, δ_H 1.02) (Table 3). Secondly, we did not observe any HMBC cross peak from H-2 [δ_H 4.53 (dd, J = 10.2, 5.4 Hz)] to C-14 (δ_C 71.9) as announced in ref. 29 indicating the location of the 14-OH in **11** was questionable. Thirdly, the location of CH_3-20 at C-13 in **11** was not only quite unreasonable but also lack of convincing evidences supporting this assignment. It should be pointed out, to the best of our knowledge, that the CH_3-20 has to be fixed at C-12 of cembranoid skeleton based on generally acknowledged rules of isoprene. Lastly, the reported structure of **11** in ref. 29 did not show any stereochemical details regarding all the chiral centers. In light of the above mentioned evidences, it is sure that the structure of sarcophytolol (**11**) was incrediblely mis-assigned and must be revised as depicted for **7**. Now, we can conclude that formally different four structures (**7** and **11**–**13**) actually are the same compound (sarcophytolol) whose correct structure is **7**.

2.2. *Anti-inflammatory activity assay of isolates **1**–**10**, **14**, **15** and **18**–**23***

Considering the interesting anti-inflammatory activity displayed by many marine cembrane-type diterpenoids,[3,32] an anti-inflammatory activity of these isolates has been tested. As shown in Table 4, compounds **1**–**4**, **8** and **19**–**23** (10 μM) displayed moderate anti-inflammatory activities in LPS-stimulated BV-2 microglial cells, among which compounds **8** and **20** were relatively more potent. Moreover, treatment with compounds **8** and **20** dose-dependently reduced the levels of pro-inflammatory cytokines IL-1β and IL-6 (Fig. 7) in LPS-stimulated BV-2 cells, which further verified their anti-inflammatory activities. In addition, all the isolates at 10 μM did not show marked cytotoxicity on BV-2 cells, suggesting that the anti-inflammatory effects of above-mentioned active compounds were not attributed to their cytotoxicity.

Since the eighteen cembranoids were tested for the biological activity, their similar structure skeleton with diverse functionalities could allow to make a preliminary structure–activity relationship (SAR) analysis. Reviewing the results of anti-inflammatory activity assay, we found that those cembranoids (**1**–**4**, **8** and **19**–**22**), all possessing a common characteristic conjugated diene moiety bearing an oxygenated group at C-14 of cembranoid framework, displayed obviously stronger activities on LPS-induced inflammatory responses in BV-2 cells than those of other tested compounds, indicating that the conjugated diene moiety bearing an oxygenated group might be responsible for the activities (Table 4).

3. Conclusion

In conclusion, although chemical investigations of the soft coral *S. glaucum* have been well documented in literatures,[3,33–35] the chemical study of this species of Ximao Island origin provides further innovative results. The notable contribution towards the advance of cembranoids

Table 3
Comparison of ^{1}H and ^{13}C NMR data of **7** with those of **11**–**13**.[a].

No.	7		11[b]		12/13[c]	
	δ_H	δ_C	δ_H	δ_C	δ_H	δ_C
1	1.32, overlap	46.7	1.33–1.34, m	46.6	1.28, m	46.5
2	4.53, dd (10.2, 4.8)	71.2	4.53, dd (10.2, 5.4)	71.1	4.51, dd (10.2, 4.8)	71.0
3	5.27, d (10.2)	125.6	5.27, d (10.2)	125.4	5.24, d (10.2)	125.4
4	–	138.8	–	138.6	–	138.5
5a	2.18, dt (12.6, 3.6)	40.1	2.18–2.21, m	39.9	2.15, m	39.9
5b	1.98, overlap		1.97–1.99, m		1.96, m	
6a	2.33, m	25.3	2.31–2.33, m	25.2	2.31, m	25.1
6b	2.11, overlap		2.11–2.12, m		2.08, m	
7	4.99, dd (10.2, 4.8)	124.2	5.00, dd (10.2, 5.4)	124.1	4.96, dd (10.2, 4.8)	123.9
8	–	136.1	–	136.0	–	135.9
9a	2.12, overlap	35.4	2.42, t (3.6)	33.7	2.07, m	35.2
9b	2.00, overlap		2.39, t (3.6)		1.97, m	
10a	1.77, m	32.0	1.75–1.77, m	18.7	1.72, m	31.6
10b	1.29, overlap		1.25–1.27, m		1.24, m	
11	3.86, d (9.6)	72.1	1.78–1.79, m 1.28–1.30, m	31.9	3.83, d (9.6)	69.9/ 72.0[d]
12	–	75.1	2.13–2.15, m 1.99–2.10, m	35.2	–	75.0
13a	2.38, dt (13.8, 3.6)	33.9	–	75.0	1.60, m	18.7
13b	1.29, overlap				1.40, m	
14a	1.63, m	18.9	3.88, d (9.6)	71.9	2.36, m	33.6
14b	1.42, m				1.22, m	
15	1.18, m	29.2	1.18–1.20, m	29.0	1.16, m	28.9
16	0.87, d (6.6)	20.9	0.88, d (6.6)	20.8	0.70, d (6.6)	20.2
17	0.72, d (6.6)	20.4	0.73, d (6.6)	20.3	0.85, d (6.6)	20.7
18	1.64, s	15.2	1.65, s	24.2	1.62, s	15.0
19	1.61, s	17.4	1.61, s	17.3	1.58, s	17.6
20	1.02, s	24.4	1.02, s	15.1	0.99, s	24.2

[a] Spectra were recorded at 600 MHz for ^{1}H NMR and 150 MHz for ^{13}C NMR. [b] Data given in ref. 29. [c] Data given in refs. 30 and 31. [d] The ^{13}C NMR data of C-11 was 69.9 in ref. 30 but that of C-11 was 72.0 in ref. 31.

chemistry is the discovery of six new cembranoids (**1**–**6**) extending the members of cembranoids family and enriching the chemical diversity of the *Sarcophyton* soft corals. Moreover, the structures of new compounds **1**–**6**, including their absolute stereochemistry, were elucidated through extensive spectroscopic analysis, quantum mechanical-NMR methods, chemical methods, as well as comparison with the reported data in the literature. It is worth noting that the wrong structure of sarcophytolol (**11**), along with very confused other related compounds **12** and **13**,[29-31] were corrected to **7** in the present work clarifying the confusions in the literature. Last but not the least, considering the increasing numbers of natural products, especially macrocyclic compounds with multiple stereogenic centers, *e.g.* cembranoids, whose structures were continuously corrected/revised in the recent years,[36–40] it raises the necessity to carefully double-check the correctness of the reported "new" natural products lacking the solid evidences of either X-ray diffraction analysis or total synthesis. In *in vitro* bioassay, the inhibitory effect screening of these isolates on LPS-induced inflammatory responses in BV-2 microglial cells led to the identification of several bioactive compounds with low cytotoxicity (the new compounds **1**–**4**, and the known ones **8** and **19**–**23**). The preliminary SAR study revealed that the conjugated diene moiety bearing an oxygenated group might be a crucial structural fragment in these bioactive cembranoids.

Table 4
The inhibitory effects of compounds **1**–**10**, **14**, **15** and **18**–**23** on LPS-induced NO production in BV-2 cells.

Compounds	NO production[a]	Cell viability[b]
1	71.32 ± 9.40*	110.60 ± 2.43
2	74.53 ± 10.18*	107.60 ± 1.04
3	74.39 ± 10.35*	97.20 ± 1.89
4	74.18 ± 7.39*	103.00 ± 4.85
5	85.28 ± 7.60	104.10 ± 2.86
6	92.67 ± 17.76	102.40 ± 2.26
7	87.23 ± 11.11	99.88 ± 2.48
8	67.77 ± 10.38**	106.30 ± 1.50
9	84.63 ± 9.06*	101.80 ± 1.77
10	82.01 ± 12.01	99.20 ± 1.36
14	85.45 ± 11.41	100.20 ± 1.46
15	80.16 ± 11.37	101.10 ± 3.19
18	88.80 ± 13.29	102.80 ± 4.88
19	77.92 ± 9.86*	101.00 ± 1.56
20	68.73 ± 7.28*	100.80 ± 2.35
21	75.92 ± 10.28*	96.05 ± 1.69
22	79.48 ± 8.85*	95.22 ± 3.51
23	76.45 ± 8.14*	105.90 ± 2.01
resveratrol (20 μM)	74.29 ± 7.39*	–

[a] NO data were normalized by mean value of LPS group, which was set to 100%; [b] Cell viability data were normalized by mean value of control group, which was set to 100%; $^{*}P < 0.05$, $^{**}P < 0.01$ *vs* the LPS group, $^{\#}P < 0.05$, $^{\#\#}P < 0.01$ *vs* the control group; $n = 3$.

4. Experimental

4.1. General experimental procedure

Optical rotations were measured on a Perkin-Elmer 241MC polarimeter (PerkinElmer, Fremont, CA, USA). IR spectra were recorded on a Nicolet 6700 spectrometer (Thermo Scientific, Waltham, MA, USA). NMR spectra were measured on Bruker Avance III 400, 500 or 600 instruments (Bruker Biospin AG, Fällanden, Germany) using TMS as an internal standard. Chemical shifts (δ) were reported in ppm with reference to the solvent signals, and coupling constants (J) were in Hz. HRESIMS spectra were recorded on an Agilent G6520 Q-TOF mass spectrometer, while HREIMS spectra were recorded on a Finnigan-MAT-95 mass spectrometer (Thermo Fisher Scientific, Waltham, USA). X-ray diffraction study was carried out on a Bruker D8 Venture diffractometer. Commercial silica gel (Qingdao Haiyang Chemical Group Co., Ltd., Qingdao, China, 200–300 and 300–400 mesh) and Sephadex LH-20 gel (Amersham Biosciences) were used for column chromatography (CC). RP-HPLC was performed on an Agilent 1260 series liquid chromatography equipped with a DAD G1315D detector and an Agilent Eclipse XDB-C_{18} column (5 μm, 9.4 × 250 mm). All solvents used for CC and HPLC were analytical grade (Shanghai Chemical Reagents Co., Ltd., Shanghai, China) and chromatographic grade (Dikma Technologies Inc., CA, USA), respectively.

4.2. Animal material

The soft coral *S. glaucum* was collected off the coast of Ximao Island, Hainan Province, China, in May 2019, at a depth of −20 m, and identified by Prof. Xiu-Bao Li from Hainan University. A voucher specimen (No. 19-XD-10) is available for inspection at Shanghai Institute of Materia Medica, Chinese Academy of Sciences.

4.3. Extraction and isolation

The frozen animals (628.7 g, dry weight) were cut into pieces and extracted with acetone at room temperature (4 × 2.5 L). The organic extract was evaporated to give a brown residue, which was then partitioned between H_2O and Et_2O. The Et_2O solution was concentrated under reduced pressure to give a dark brown residue (51.0 g), half of

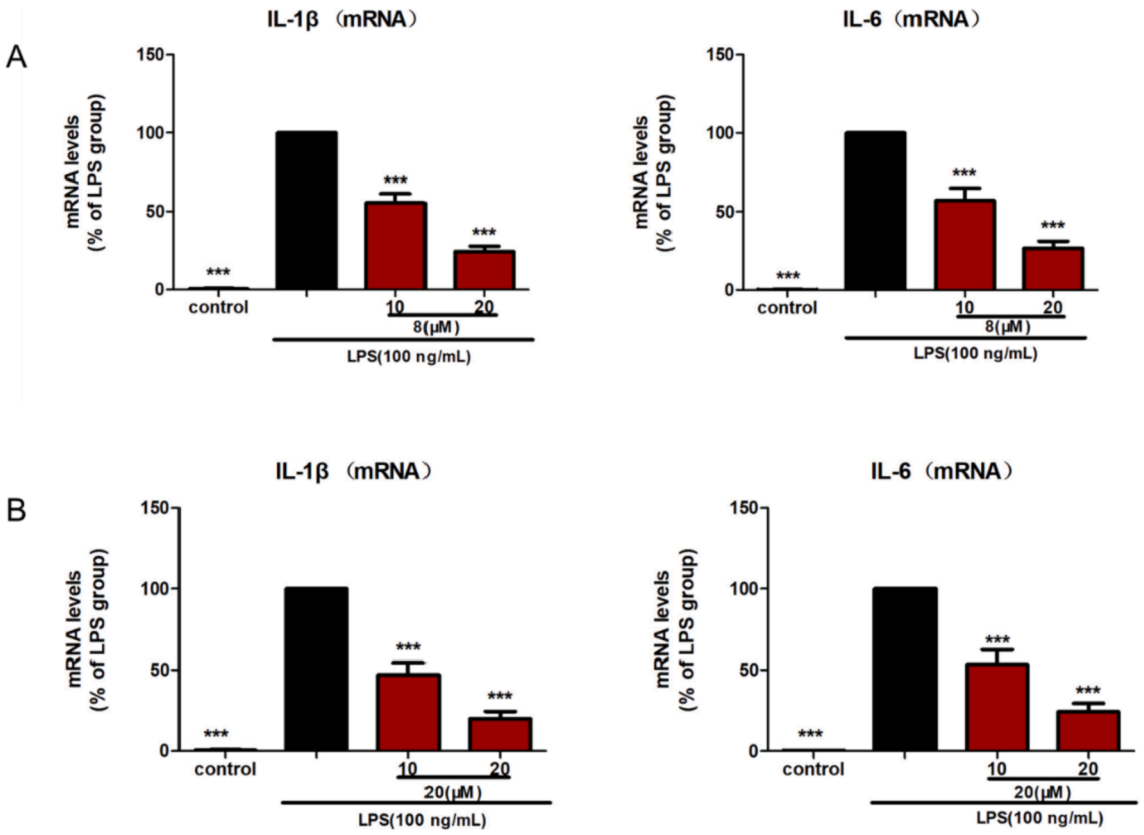

Fig.7. Compounds **8** (A) and **20** (B) reduced the levels of pro-inflammatory cytokines IL-1β and IL-6 in LPS-treated BV-2 microglial cells. Data were normalized by LPS group, and presented as Means ± SEM, $n = 4$. ***$p < 0.001$ *vs* the LPS group.

which was fractionated by gradient Si gel (200–300 mesh) column chromatography (CC) [0 → 100% Et_2O in petroleum ether (PE)], yielding six fractions (A−F). The fractions A−D were then fractionated into subfractions by Sephadex LH-20 [PE/CH_2Cl_2/MeOH (2:1:1)], respectively. The subfraction A2 (122.0 mg) was separated on a column of silica gel (0 → 30% Et_2O in PE) to afford **8** (66.0 mg), **14** (2.8 mg) and **16** (12.4 mg). The subfraction B3 (162.0 mg) was purified by RP-HPLC [MeOH/H_2O (92:8), 3.0 mL/min], yielding compounds **10** (2.5 mg, t_R = 9.9 min), **15** (3.5 mg, t_R = 15.3 min), **23** (2.0 mg, t_R = 16.0 min) and **24** (5.0 mg, t_R = 17.2 min). The subfraction B4 (100.5 mg) was separated by RP-HPLC [MeCN/H_2O (82:18), 3.0 mL/min] to afford **18** (2.8 mg, t_R = 23.3 min). Followed by silica gel CC [PE/Et_2O (30:1 to 1:1)], three mixtures C4b, C4c and C4d were obtained from subfraction C4 (620.0 mg). The subfraction C4b (55.0 mg) was further purified by RP-HPLC [MeOH/H_2O (84:16), 3.0 mL/min, respectively] to give compounds **7** (8.5 mg, t_R = 13.3 min), **19** (11.0 mg, t_R = 14.3 min) and **17** (3.1 mg, t_R = 21.1 min). Like subfraction C4b, each of subfractions C4c (148.0 mg) and C4d (68.1 mg) was separated by RP-HPLC [MeOH/H_2O (82:18) and MeOH/H_2O (90:10), respectively] to yield **6** (1.5 mg, t_R = 12.8 min), **2** (1.6 mg, t_R = 15.5 min), **3** (3.7 mg, t_R = 19.3 min), **1** (13.0 mg, t_R = 9.0 min), **20** (20.6 mg, t_R = 10.0 min) and **22** (2.5 mg, t_R = 16.8 min), respectively. The subfraction C6 (68.1 mg) was purified by RP-HPLC [MeOH/H_2O (84:16), 3.0 mL/min], yielding compounds **9** (2.8 mg, t_R = 5.9 min), **21** (1.8 mg, t_R = 7.5 min), **5** (1.2 mg, t_R = 8.5 min) and **4** (3.0 mg, t_R = 14.7 min).

Ximaoglaucumin A ***(1)***: colorless oil; $[\alpha]^{20}_D$ + 221.1 (*c* 0.42, MeOH); UV (MeCN) λ_{max} (log ε) 251.0 (4.06) nm; ECD [MeCN, λ ($\Delta\varepsilon$), *c* 0.4]: 247.0 (+11.51) nm; IR ν_{max} 3440, 2955, 2920, 1738, 1439, 1372, 1236, 1022 cm^{-1}; ^1H and ^{13}C NMR data, see Tables 1 and 2; HRESIMS *m/z* 369.2409 ([M + Na]$^+$, calcd for $C_{22}H_{34}NaO_3$, 369.2400).

(S)-MTPA ester of ***1*** *(**1a**)*: ^1H NMR (pyridine-d_5, 400 MHz): δ_H 6.520 (1H, d, J = 11.6 Hz, H-2), 6.450 (1H, d, J = 11.6 Hz, H-3), 4.993 (1H, brs, H-7), 5.543 (1H, t, J = 5.2 Hz, H-11), 2.837 (1H, m, H-13a), 2.837 (1H, m, H-13b), 2.591 (1H, m, H-15), 1.157 (3H, d, J = 6.8 Hz, H-16), 1.098 (3H, d, J = 6.8 Hz, H-17), 1.749 (3H, s, H-18), 1.407 (3H, s, H-19), 4.788 (1H, d, J = 12.0 Hz, H-20a), 4.678 (1H, d, J = 12.0 Hz, H-20b), 2.057 (3H, s, OAc).

(R)-MTPA ester of ***1*** *(**1b**)*: ^1H NMR (pyridine-d_5, 400 MHz): δ_H 6.484 (2H, brs, H-2 and H-3), 5.006 (1H, brs, H-7), 5.531 (1H, t, J = 6.8 Hz, H-11), 2.938 (1H, m, H-13a), 2.852 (1H, m, H-13b), 2.499 (1H, m, H-15), 1.057 (3H, d, J = 6.8 Hz, H-16), 0.946 (3H, d, J = 6.8 Hz, H-17), 1.738 (3H, s, H-18), 1.409 (3H, s, H-19), 4.823 (1H, d, J = 12.0 Hz, H-20a), 4.712 (1H, d, J = 12.0 Hz, H-20b), 2.076 (3H, s, OAc).

Ximaoglaucumin B ***(2)***: colorless oil; $[\alpha]^{20}_D$ + 174.2 (*c* 0.15, MeOH); UV (MeCN) λ_{max} (log ε) 251.0 (4.11) nm; ECD [MeCN, λ ($\Delta\varepsilon$), *c* 0.5]: 247.5 (+10.16) nm; IR ν_{max} 3444, 2959, 2925, 2855, 1738, 1444, 1371, 1259, 1018 cm^{-1}; ^1H and ^{13}C NMR data, see Tables 1 and 2; HREIMS *m/z* 346.2497 (M^+, calcd for $C_{22}H_{34}O_3$, 346.2502).

Ximaoglaucumin C ***(3)***: colorless oil; $[\alpha]^{20}_D$ + 51.8 (*c* 0.35, MeOH); UV (MeCN) λ_{max} (log ε) 250.0 (4.03) nm; ECD [MeCN, λ ($\Delta\varepsilon$), *c* 0.6]: 248.5 (+7.74) nm; IR ν_{max} 3446, 2962, 2926, 1738, 1446, 1372, 1238, 1022 cm^{-1}; ^1H and ^{13}C NMR data, see Tables 1 and 2; HREIMS *m/z* 346.2509 (M^+, calcd for $C_{22}H_{34}O_3$, 346.2502).

Ximaoglaucumin D ***(4)***: colorless oil; $[\alpha]^{20}_D$ + 67.7 (*c* 0.30, MeOH); UV (MeCN) λ_{max} (log ε) 249.5 (3.70) nm; ECD [MeCN, λ ($\Delta\varepsilon$), *c* 0.7]: 247.5 (+4.47) nm; IR ν_{max} 3386, 2958, 2930, 2869, 1444, 1383, 1047 cm^{-1}; ^1H and ^{13}C NMR data, see Tables 1 and 2; HRESIMS *m/z* 343.2245 ([M + Na]$^+$, calcd for $C_{20}H_{32}NaO_3$, 343.2244).

Ximaoglaucumin E ***(5)***: colorless oil; $[\alpha]^{20}_D$ + 70.0 (*c* 0.12, MeOH); UV (MeCN) λ_{max} (log ε) 249.0 (3.74) nm; ECD [MeCN, λ ($\Delta\varepsilon$), *c* 0.6]: 245.0 (+3.73) nm; IR ν_{max} 3438, 2957, 2925, 2868, 1446, 1383, 1039, 973 cm^{-1}; ^1H and ^{13}C NMR data, see Tables 1 and 2; HRESIMS *m/z* 343.2252 ([M + Na]$^+$, calcd for $C_{20}H_{32}NaO_3$, 343.2244).

Ximaoglaucumin F ***(6)***: colorless oil; $[\alpha]^{20}_D$ –121.4 (*c* 0.14, MeOH);

ECD [MeCN, λ ($\Delta\varepsilon$), c 0.5]: 209.0 (–19.23) nm; IR ν_{max} 3452, 2962, 2926, 2872, 1737, 1440, 1371, 1260, 1084, 1023 cm^{-1}; ^1H and ^{13}C NMR data, see Tables 1 and 2; HREIMS m/z 362.2456 (M^+, calcd for $C_{22}H_{34}O_4$,362.2452).

*Sarcophytolol (**7**)*: colorless oil; $[\alpha]^{20}_D$ + 126.5 (c 0.42, MeOH); ECD [MeCN, λ ($\Delta\varepsilon$), c 0.7]: 206.0 (+13.58) nm; IR ν_{max} 3441, 2940, 2869, 1448, 1383, 1023, 982 cm^{-1}; ^1H and ^{13}C NMR data, see Table 3; HRESIMS m/z 307.2636 ($[M + H]^+$, calcd for $C_{20}H_{35}O_2$, 307.2632).

*Sarcophytol R (**25**)*: colorless oil; ^1H NMR data, see Table S2; HRESIMS m/z 327.2299 ($[M + Na]^+$, calcd for $C_{20}H_{32}NaO_2$, 327.2295)..

*Sarcophytol E (**26**)*: colorless oil; $[\alpha]^{20}_D$ + 80.2 (c 0.30, MeOH); ^1H and ^{13}C NMR data, see Table S2; HRESIMS m/z 327.2290 ($[M + Na]^+$, calcd for $C_{20}H_{32}NaO_2$, 327.2295).

4.4. X-ray crystallographic analysis

Compound **8** was crystallized from PE/CH_2Cl_2/MeOH (2:1:1) at RT. The crystallographic data for **8** was collected on a Bruker D8 Venture diffractometer equipped with Cu Kα radiation (λ = 1.54178 Å). The collected data integration and reduction were processed with SAINT V8.37A software, and multi-scan absorption corrections were performed using the SADABS program. The structure was solved by using ShelXTL and refined on F^2 by the full-matrix least-squares technique using the SHELXL-2015 program package. The crystallographic data has been uploaded to the Cambridge Crystallographic Data Centre with CCDC number 2033870. The data can be obtained free of charge via www.ccdc.cam.ac.uk/data_request/cif. Details of these crystallographic data were shown in Table S3.

4.5. Computational section

Conformational search was accomplished using the torsional sampling (MCMM) method and OPLS_2005 force field with the conformational search using an energy window of 21 kJ/mol. Conformers above 1% Boltzmann populations were subjected to NMR calculations. DFT calculations were performed using Gaussian 09. Structure optimizations were done at the B3LYP/6-31G* level of theory. Magnetic shielding constants (σ) were calculated by means of the gauge including atomic orbitals (GIAO) method at the PCM/mPW1PW91/6-31G+** levels of theory, as recommended for DP4 +. Finally, shielding constants were averaged over the Boltzmann distribution obtained for each stereoisomer and correlated with the experimental data.

4.6. In vitro anti-inflammatory assay

BV-2 microglia cells (2.0 × 10^5 cells/mL) were cultured in 96-well plates with DMEM high-glucose medium containing 10% fetal bovine serum in a humidified, 37 °C, 5% CO_2-containing incubator for 24 h. To assess the *in vitro* anti-inflammatory effects of test compounds, BV-2 cells were then pretreated with 10 μM of test compounds for 2 h, followed by 100 ng/mL of LPS exposure for 24 h. The culture medium of each well (50 μL) was collected, and then incubated with 50 μL of Greiss buffer (Sigma-Aldrich, St.Louis, MO, USA) for 15 min at room temperature. The absorbance of mixture was measured at 540 nm using a microplate reader, and the level of nitrite was calculated from a standard curve of sodium nitrite.

To further verify the anti-inflammatory effects of potent active compounds, the levels of pro-inflammatory cytokines IL-1β and IL-6 of BV-2 cells were measured. BV-2 cells (1 × 10^5 cells/mL) were cultured in 12 well plates. Cells were pretreated compounds **8** and **20** for 2 h, and further incubated with LPS (100 ng/mL) for 6 h. Total RNAs were then extracted from BV-2 cells by using Trizol reagent (Invitrogen) and reverse transcribed into cDNAs using PrimeScript Mater kit (Takara). Real-time PCR amplification of the cDNAs was performed using Taqman SYBR kit (Takara) according to the manufacturer's protocol, with GAPDH as internal reference gene.

Student's t test was used to compare data between two groups. One-way analysis of variance followed by Dunnett's multiple comparison test was used for comparisons between multiple groups.

4.7. Cell viability determination

For measurement of the influence of isolates on cell viabilities, BV-2 cells were seeded at a density of 1.25 × 10^4 cells/mL into 96-well plates with 100 μL/well and maintained in a humidified atmosphere of 5% CO_2 and 95% air at 37 °C. Twenty-four hours after seeding, the cells were treated with 10 μM of test compounds for another 24 h, and then treated with 0.5 mg/mL MTT for 3 h. The absorbance value at 490 nm was measured by a microplate reader (Molecular Devices, Sunnyvale, CA, USA) and the cell viability was calculated.

Declaration of Competing Interest

The authors declare that they have no known competing financial interests or personal relationships that could have appeared to influence the work reported in this paper.

Acknowledgements

This work was financially supported by the Natural Science Foundation of China (No. 81991521), the National Key Research and Development Program of China (No. 2018YFC0310903), the Science and Technology Commission of Shanghai Municipality (No. 18430712500), the Drug Innovation Major Project (No. 2018ZX09711-001-001-009) and the SKLDR/SIMM Project (No. SIMM2013ZZ-06).

Appendix A. Supplementary data

Supplementary data to this article can be found online at https://doi.org/10.1016/j.bmc.2021.116139.

References

1 Ne'eman I, Fishelson L, Sarcophine Kashman Y. New toxin from the soft coral *Sarcophyton glaucum* (Alcyonaria). *Toxicon*. 1974;12:593–598.
2 Zhang W, Guo Y-W, Gu Y-C. Secondary metabolites from the South China Sea invertebrates: Chemistry and biological activity. *Curr Med Chem*. 2006;13:2041–2090.
3 Liang L-F, Guo Y-W. Terpenes from the soft corals of the genus *Sarcophyton*: Chemistry and biological activities. *Chem Biodivers*. 2013;10:2161–2196.
4 Zhou Z-F, Menna M, Cai Y-S, et al. Polyacetylenes of marine origin: Chemistry and bioactivity. *Chem Rev*. 2015;115:1543–1596.
5 Jiang C-S, Muller Werner EG, Schroder Heinz C, et al. Disulfide- and multisulfide-containing metabolites from marine organisms. *Chem Rev*. 2012;112:2179–2207.
6 Li G, Li H, Tang W, et al. Klyflaccilides A and B, diterpenoids with 6/5/8/3 fused tetracyclic carbon skeleton from the Hainan soft coral *Klyxum flaccidum*. *Org Lett*. 2019;21:5660–5664.
7 Ye F, Zhu Z-D, Chen J-S, et al. Xishacorenes A-C, diterpenes with bicyclo[3.3.1]nonane nucleus from the Xisha soft coral *Sinularia polydactyla*. *Org Lett*. 2017;19:4183–4186.
8 Li S-W, Ye F, Zhu Z-D, et al. Cembrane-type diterpenoids from the South China Sea soft coral *Sarcophyton mililatensis*. *Acta Pharm. Sin. B*. 2018;8:944–955.
9 Ye F, Li J, Wu Y, et al. Sarinfacetamides A and B, nitrogenous diterpenoids with tricyclo[6.3.1.01,5]dodecane scaffold from the South China Sea soft coral *Sarcophyton infundibuliforme*. *Org Lett*. 2018;20:2637–2640.
10 Liang L-F, Kurtan T, Mandi A, et al. Unprecedented diterpenoids as a PTP1B inhibitor from the Hainan soft coral *Sarcophyton trocheliophorum* Marenzeller. *Org Lett*. 2013;15:274–277.
11 Yang M, Li X-L, Wang J-R, et al. Sarcomililate A, an unusual diterpenoid with tricyclo[11.3.0.02,16]hexadecane carbon skeleton, and its potential biogenetic precursors from the Hainan soft coral *Sarcophyton mililatensis*. *J Org Chem*. 2019;84:2568–2576.
12 Jia R, Kurtan T, Mandi A, et al. Biscembranoids formed from an α, β-unsaturated γ-lactone ring as a dienophile: Structure revision and establishment of their absolute configurations using theoretical calculations of electronic circular dichroism spectra. *J Org Chem*. 2013;78:3113–3119.
13 Yao L-G, Liu H-L, Guo Y-W, et al. New cembranoids from the Hainan soft coral *Sarcophyton glaucum*. *Helv Chim Acta*. 2009;92:1085–1091.
14 Kobayashi M, Nakagawa T, Mitsuhashi H. Marine terpenes and terpenoids. I. Structures of four cembrane-type diterpenes; sarcophytol-A, sarcophytol-A acetate sarcophytol-B, and sarcophytonin-A, from the soft coral, *Sarcophyton glaucum*. *Chem Pharm Bull*. 1979;27:2382–2387.

15 Kobayashi M, Osabe K. Marine terpenes and terpenoids. VII. Minor cembranoid derivatives, structurally related to the potent anti-tumor-promoter sarcophytol A, from the soft coral *Sarcophyton glaucum*. *Chem Pharm Bull*. 1989;37:631–636.
16 Kobayashi M, Kondo K, Osabe K, et al. Marine terpenes and terpenoids. V. Oxidation of sarcophytol A, a potent anti-tumor-promoter from the soft coral *Sarcophyton glaucum*. *Chem Pharm Bull*. 1988;36:2331–2341.
17 Peniston M, Rodriguez AD. The isolation of (-)-sarcophytola and (+)-marasol from the Caribbean gorgonian *Plexaura flexuosa*. *J Nat Prod*. 1991;54:1009–1016.
18 Kinamoni Z, Groweiss A, Carmely S, et al. Several new cembranoid diterpenes from three soft corals of the Red Sea. *Tetrahedron*. 1983;39:1643–1648.
19 Iguchi K, Shimura H, Yamada Y. New cembrane-type diterpenoids from the Okinawan soft coral *Sinularia* sp. *J Nat Prod*. 1992;55:1779–1782.
20 Ahmed AF, Wen Z-H, Su J-H, et al. Oxygenated cembranoids from a Formosan soft coral *Sinularia gibberosa*. *J Nat Prod*. 2008;71:179–185.
21 Raldugin VA, Yaroshenko NI, Shakirov MM. Oxidative transformations of cembrane diterpenoids. V. Reaction of cembrene with N-bromosuccinimide in aqueous acetone. *Khim Prir Soedin*. 1983;19:150–158.
22 Rahelivao MP, Gruner M, Luebken T, et al. Chemical constituents of the soft corals *Sinularia vanderlandi* and *Sinularia gravis* from the coast of Madagascar. *Org Biomol Chem*. 2016;14:989–1001.
23 Seco JM, Quinoa E, Riguera R. The assignment of absolute configuration by NMR. *Chem Rev*. 2004;104:17–117.
24 Kobayashi M, Iesaka T, Nakano E. Marine terpenes and terpenoids. IX. Structures of six new cembranoids, sarcophytols F, K, P, Q, R and S, from the soft coral *Sarcophyton glaucum*. *Chem. Pharm. Bull.* 1989;37:2053–2057.
25 Nakagawa T, Kobayashi M, Hayashi K, et al. Marine terpenes and terpenoids. II. Structures of three cembrane-type diterpenes, sarcophytol-C, sarcophytol-D, and sarcophytol-E, from the soft coral, *Sarcophyton glaucum*. *Chem Pharm Bull*. 1981;29:82–87.
26 Li S-W, Cuadrado C, Yao L-G, et al. Quantum Mechanical-NMR-Aided configuration and conformation of two unreported macrocycles isolated from the soft coral *Lobophytum sp.*: Energy calculations versus coupling constants. *Org Lett*. 2020;22:4093–4096.
27 Grimblat N, Zanardi MM, Sarotti AM. Beyond DP4: An improved probability for the stereochemical assignment of isomeric compounds using quantum chemical calculations of NMR shifts. *J Org Chem*. 2015;80:12526–12534.
28 Sun L-L, Li W-S, Li J, et al. Uncommon diterpenoids from the South China Sea soft coral *Sinularia humilis* and their stereochemistry. *J Org Chem*. 2021;86:3367–3376.
29 Al-Lihaibi SS, Alarif WM, Abdel-Lateff A, et al. Three new cembranoid-type diterpenes from Red Sea soft coral *Sarcophyton glaucum*: isolation and antiproliferative activity against HepG2 cells. *Eur J Med Chem*. 2014;81:314–322.
30 Al-Footy KO, Alarif WM, Asiri F, et al. Rare pyrane-based cembranoids from the Red Sea soft coral *Sarcophyton trocheliophorum* as potential antimicrobial-antitumor agents. *Med Chem Res*. 2015;24:505–512.
31 Hamed A, Issa MY, Ghani MA, et al. Crystal structure and configuration revision of 9-hydroxy-7,8-dehydro-sarcotrocheliol and sarcotrocheliol. *Nat Prod Res*. 2019;33:3029–3032.
32 Wu Q-H, Li X-W, Li H, et al. Bioactive polyoxygenated cembranoids from a novel Hainan chemotype of the soft coral *Sinularia flexibilis*. *Bioorg Med Chem Lett*. 2019;29:185–188.
33 Zhang J, Tang X-L, Han X, et al. Sarcoglaucins A-I, new antifouling cembrane-type diterpenes from the South China Sea soft coral *Sarcophyton glaucum*. *Org Chem Front*. 2019;6:2004–2013.
34 Chao C-H, Li W-L, Huang C-Y, et al. Isoprenoids from the soft coral *Sarcophyton glaucum*. *Mar Drugs*. 2017;15:1–11.
35 Huang C-Y, Sung P-J, Uvarani C, et al. Glaucumolides A and B, biscembranoids with new structural type from a cultured soft coral *Sarcophyton glaucum*. *Sci Rep*. 2015;5:15624.
36 Sun D-Y, Han G-Y, Gong J-X, et al. Asymmetric total synthesis of distaminolyne A and revision of its absolute configuration. *Org Lett*. 2017;19:714–717.
37 Li G, Li H, Zhang Q, et al. Rare cembranoids from Chinese soft coral *Sarcophyton ehrenbergi*: Structural and stereochemical studies. *J Org Chem*. 2019;84:5091–5098.
38 Shen S-M, Li H, Wang J-R, et al. Further new complex daphniphyllum alkaloids from the stems and leaves of *Daphniphyllum calycinum*: Structure and stereochemistry. *Tetrahedron*. 2020;76, 131616.
39 Nicolaou KC, Snyder Scott A. Chasing molecules that were never there: misassigned natural products and the role of chemical synthesis in modern structure elucidation. *Angew Chem Int Ed*. 2005;44:1012–1044.
40 Wu J, Lorenzo P, Zhong S, et al. Synergy of synthesis, computation and NMR reveals correct baulamycin structures. *Nature*. 2017;547:436–440.